

Reshaping Nanocrystals for Tunable Plasmonic Substrates

Minjung Kim,[†] Young Wook Lee,[†] Dongheun Kim,[‡] Seunghoon Lee,[†] Soo-Ryoon Ryoo,[†] Dal-Hee Min,[§] Sang Bok Lee,^{‡,⊥} and Sang Woo Han^{*,†}

[†]Department of Chemistry and KI for the NanoCentury, KAIST, Daejeon 305-701, Korea

[‡]Graduate School of Nanoscience and Technology (WCU), KAIST, Daejeon 305-701, Korea

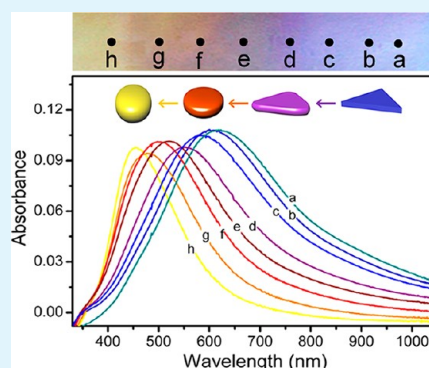
[§]Department of Chemistry, Seoul National University, Seoul 151-747, Korea

[⊥]Department of Chemistry and Biochemistry, University of Maryland, College Park, Maryland 20742, United States

S Supporting Information

ABSTRACT: Plasmonic nanostructures with tunable optical properties and their designed spatial arrangements can facilitate a variety of application ranging from plasmonics to biosensors with unprecedented sensitivity. Here we describe a facile and versatile method for fabricating tunable plasmonic substrates based on the reshaping of metal nanocrystals. Anisotropic etching and redeposition of Ag atoms mediated by halide ions transformed Ag nanoprisms deposited on two- or three-dimensional surfaces or in solution into nanostructures with an oblate spheroidal shape, and corresponding localized surface plasmon resonances features could be tuned. The reshaping nanocrystal strategy can even facilitate the preparation of new classes of plasmonic substrates with gradient or patterned plasmonic properties, which cannot be realized easily using existing lithographic techniques. The substrates with gradient plasmonic properties can serve as platforms for tunable surface-enhanced Raman scattering.

KEYWORDS: nanoprisms, plasmonic nanostructures, Raman spectroscopy, reshaping nanocrystal, silver



INTRODUCTION

Metal nanocrystals (NCs) have drawn tremendous research interest recently due to their promising applications in catalysis, sensors, plasmonics, and electronic devices.^{1–3} Among the metal NCs, Ag and Au crystals have been of particular interest as optical materials because they exhibit distinctive optical properties due to localized surface plasmon resonances (LSPR), which are collective oscillations of free electrons that can be strongly coupled to incident electromagnetic fields.^{4–6} The morphology of NCs and their spatial organization explicitly determine the plasmonic characteristics, such as the LSPR profile and surface-enhanced Raman scattering (SERS) efficiency.^{7–9} Accordingly, several strategies have been developed for preparing metal NCs with well-defined geometries and for constructing two- (2D) and three-dimensional (3D) assemblies of NC building blocks with ordered structures. However, the lack of simple and versatile methods for preparing plasmonic structures with designed properties and spatial regularity has slowed the adaptation of these unique plasmonic structures to practical applications. For instance, the preparation of a range of structures is required to span a wide range of LSPR wavelengths, which demand precisely controlled synthetic conditions that are usually difficult to reproduce.

Recently, NC reshaping strategies have provided a promising route to systematically tuning the plasmonic properties of NCs. This so-called “backward tuning” provides better controllability than the “forward tuning” approach, which relies on control

over the shapes of nanostructures during the nucleation/growth processes by controlling the synthesis parameters.¹⁰ The backward tuning approach thereby generates stable NCs with a wide range of LSPR wavelengths. Through chemical etching, UV irradiation, pH control, and thermal treatment, NCs with tunable plasmonic characteristics were synthesized from Ag nanoplates,^{11–15} Au nanorods,^{16,17} branched Au NCs,^{18,19} and Ag nanooctahedra.¹⁰ In this work, we show that NC reshaping strategy can produce systematically tunable plasmonic structures on versatile 2D and 3D substrates as well as in solution under low-temperature, mild chemical conditions. In our approach, Ag nanostructures with controlled plasmonic properties can be formed by reconstructing Ag NCs with a prism-like morphology (Ag nanoprisms, AgNPs) using a halide ion-induced anisotropic etching method.^{11,12,15,18} Furthermore, 2D or 3D substrates with gradient LSPR features and large-area patterned plasmonic substrates can be readily fabricated based on this protocol, surpassing the limitations of traditional lithographic processes. These types of tunable plasmonic substrates can be applied as a new class of platforms in optical applications such as SERS-based sensing.

Received: July 30, 2012

Accepted: August 9, 2012

Published: August 9, 2012

EXPERIMENTAL SECTION

Chemicals and Materials. AgNO₃ (Aldrich), NaBH₄ (Aldrich), trisodium citrate dihydrate (Aldrich), H₂O₂ (Aldrich), poly(vinyl pyrrolidone) (PVP, MW = 55 000, Aldrich), 3-aminopropyltrimethoxysilane (3-APTMS, Aldrich), 4-aminobenzenethiol (4-ABT, Aldrich), poly(dimethylsiloxane) (PDMS) prepolymer (Sylgard 184, Dow Corning Corp.), and (tridecafluoro-1,1,2,2-tetrahydrooctyl)-trichlorosilane (United Chemical Technologies, Inc.) were used as received. Other chemicals, unless specified, were reagent grade, and highly purified deionized water with a resistivity of greater than 18.0 MΩ cm was used in the preparation of aqueous solutions.

Synthesis of AgNPs. AgNPs were prepared by the reduction of AgNO₃ with NaBH₄ in the presence of citrate and H₂O₂.^{20,21} AgNO₃ was initially dissolved in distilled water (0.1 mM, 25 mL), and the solution was stirred vigorously. An aqueous solution of trisodium citrate dihydrate (30 mM, 1.5 mL), PVP (5 mg/mL, 1.5 mL), and H₂O₂ (28 wt %, 60 μL) were added to the AgNO₃ solution. To the mixture, an aqueous solution of NaBH₄ (100 mM, 300 μL) was quickly injected, forming a colloid that was pale yellow in color. After 10 min, the color of the colloid continued to change from yellow to blue. The reaction was performed at room temperature. The resultant AgNPs were centrifuged (9000 rpm for 30 min) and redispersed in water to remove the excess reactants in the solution.

Reshaping of the AgNPs. In a typical experiment for reshaping the AgNPs in solution, an aqueous solution of NaBr with various concentrations was added into an as-prepared AgNP solution with a 1:1 (v/v) ratio. For reshaping the AgNPs on substrates, the AgNPs were assembled on the amine-terminated substrates such as Si wafers, microscope slide and cover glasses, indium–tin oxide (ITO) glasses, and silica gel (particle size = 63–200 μm). The amine-terminated substrates were prepared as follows. The bare substrates were pretreated with Piranha solution (H₂O₂:H₂SO₄ = 1:3, v/v) (*Caution: Piranha solution is a very strong oxidizing agent and extremely dangerous. It should be handled with great care.*) for 1–2 h. Then the substrates were immersed in an ethanol solution of 1% 3-APTMS in the presence of 0.1% acetic acid for 5 h. The modified substrates were rinsed thoroughly with deionized water. To assemble the AgNPs on the substrates, we dipped the amine-terminated substrates into the AgNPs solution for 12 h. To prepare the substrates with a gradient of color, the AgNP-modified substrates were dipped into a NaBr solution (1.0 × 10⁻⁶ M) with maintaining a steady speed (41 mm h⁻¹), which was controlled by a syringe pump (Cole-Parmer). In the experiments, the substrates were attached to the moving bar of the syringe pump. For the production of tunable plasmonic three-dimensional substrates, AgNP-coated silica gel was packed into a syringe, whose diameter was 7 mm. The passage of an aqueous NaBr solution (1.0 × 10⁻⁶ M, 1 mL) through AgNP-coated silica gel column resulted in a gradient of color along the column.

Preparation of Patterned Plasmonic Substrates. For patterned reshaping of AgNPs, microcontact printing (μCP) technique was employed. To prepare the PDMS stamp, a PDMS prepolymer was cast against a microfabricated photoresist master (50 μm circular wells separated by 150 or 50 μm trenches separated by 200 μm). Curing the prepolymer at 60 °C for 12 h and peeling it away from the master provided a negative replica of the two-dimensional pattern of the photoresist. The negative replica of PDMS, composed of protruding cylindrical or line features on the surface, was used as a stamp. Before casting the PDMS prepolymer, the master was pretreated with (tridecafluoro-1,1,2,2-tetrahydrooctyl)trichlorosilane for 1 h under vacuum at room temperature to functionalize the surface with the fluorocarbon. The PDMS stamp was inked by drop casting of an ethanol solution of 0.5 mM NaBr. The stamp was brought into contact with the AgNP-modified cover glass for 1 min. The stamp was then carefully peeled off, and the substrate was washed with deionized water and dried in the air.

Instrumentation. The extinction spectra were recorded using a UV–vis absorption spectrometer (Agilent 8453). Transmission electron microscopy (TEM) images were obtained using a JEOL JEM-2010 transmission electron microscope operating at 200 kV after

placing a drop of hydrosol on carbon-coated Cu grids (200 mesh). High-resolution TEM (HRTEM) characterizations were performed using a FEI Tecnai G2 F30 Super-Twin transmission electron microscope operating at 300 kV. Scanning electron microscopy (SEM) images of the samples were taken using a FEI field-emission scanning electron microscope (FESEM, Phillips Model XL30 S FEG). X-ray photoelectron spectroscopy (XPS) measurements were carried out using a VG Scientific ESCALAB 250 spectrometer with Al Kα X-ray (1486.6 eV) as the light source. The base pressure of the chamber was ~1 × 10⁻¹⁰ Torr and the electron takeoff angle was 90°. For SERS measurements, a nanostructure-modified substrate was soaked in a 1 mM 4-ABT solution in ethanol for 30 min. After the substrate was taken out, it was washed with ethanol and dried under ambient condition. Raman spectra were obtained using a Jobin Yvon/Horiba LabRAM spectrometer equipped with an integral microscope (Olympus BX 41). The 514.5 nm radiation from an air-cooled argon ion laser and the 632.8 nm from an air-cooled He/Ne laser were used as the excitation sources. The Raman band of a silicon wafer at 520 cm⁻¹ was used to calibrate the spectrometer. SERS spectra were obtained from more than 10 different spots for 5 different samples. The peak intensities at specific excitation wavelengths were all normalized with respect to that of the Raman band of a silicon wafer. Optical micrographs of the patterned substrates were obtained using an Olympus BX51 M optical microscope.

RESULTS AND DISCUSSION

AgNPs were prepared in aqueous solutions according to previously reported methods.^{20,21} The synthesized nanostructures were mainly triangular in shape with an average edge length and thickness of 33 and 4.5 nm, respectively (Figure S1a in the Supporting Information). The colloidal solution of AgNPs exhibited a distinct blue color and showed three LSPR peaks at 660 (strong), 470 (medium), and 332 nm (weak but sharp) in the UV–vis spectrum (see Figure S1b in the Supporting Information). These peaks could be assigned to in-plane dipole, in-plane quadrupole, and out-of-plane quadrupole resonances, respectively.^{22,23} Noticeably, the color of the AgNP solution changed dramatically from blue to yellow within 15 min upon addition of NaBr (to a final concentration of 4.0 × 10⁻⁶ M, Ag/NaBr molar ratio = 20:1), as shown in Figure 1a. The color changes in the AgNP solution was also in accord with the changes in the UV–vis spectral features (Figure 1b). As the reaction time increased, the in-plane dipole LSPR peak gradually blue-shifted, and after 15 min, only two LSPR peaks were observed at 437 (strong) and 357 nm (medium). The time required to complete the color and spectral changes depended on the amount of NaBr added to the AgNP solution. For instance, it took 300, 90, and 15 s for the color change to go to completion when the final concentrations of NaBr were, respectively, 1.0 × 10⁻⁵, 1.0 × 10⁻⁴, and 1.0 × 10⁻³ M. These findings suggested that a specific structural change took place among the AgNPs. The process of reshaping the AgNPs was monitored by TEM measurements at different reaction times (Figure 1c). During the early stages of the reaction, the corners of the AgNPs were slightly rounded, and the thickness of the AgNPs increased. As the reaction time increased, AgNPs became more rounded and their thickness increased. The AgNPs finally transformed into nanostructures with an oblate spheroidal shape. The average lengths of the long and short symmetry axes of Ag nanooblates (AgNOs) were 20.7 and 15.3 nm, respectively. The two LSPR peaks that appeared at 437 and 357 nm in the UV–vis extinction spectra of the hydrosol after NaBr treatment were thus assigned, respectively, to the longitudinal and transverse resonance modes of the AgNOs.²⁴

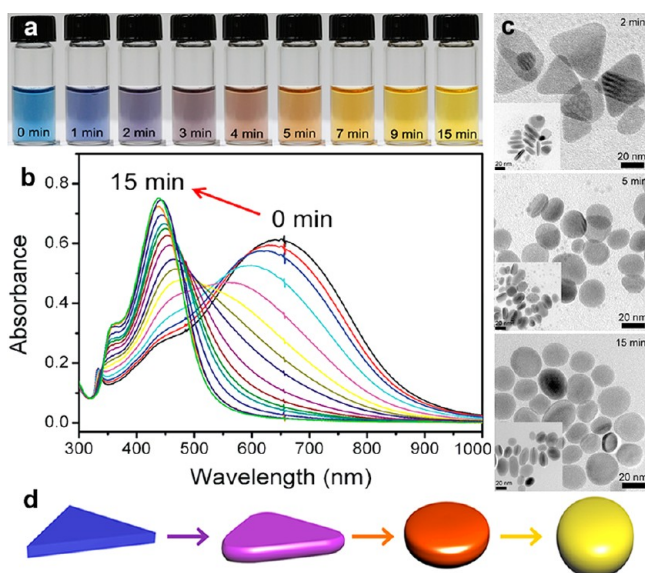


Figure 1. (a) Digital photographs and (b) successive extinction spectra (1 min interval) of a colloidal solution of AgNPs incubated for different lengths of time after addition of NaBr. (c) TEM images of Ag nanostructures collected at different reaction times. From the TEM images of some Ag nanostructures vertically aligned on the TEM grids shown in each inset, the mean thickness of Ag nanostructures could be estimated. (d) Schematic illustration of the reshaping of AgNPs induced by NaBr treatment.

The nanostructure shape transformation was attributed to anisotropic etching of the AgNPs by Br^- ions. AgNPs are bound by two low-energy $\{111\}$ facets at the top and bottom faces, and the side faces are enclosed by $\{100\}$ and $\{110\}$ facets and contain twin defects and stacking faults lying parallel to the basal planes.^{22,23,25} The twin defects and stacking faults, as well as the corners of AgNPs have a lower coordination number than the $\{111\}$ -faceted basal planes and, therefore, a higher surface energy. Ag atoms at these energetic sites, especially in the corner regions, were very reactive toward chemical etching with halide ions, and these atoms preferentially dissociated from the AgNPs by forming coordination complexes with halide ions.^{11,12,26} These unstable complexes formed small clusters and subsequently redeposited onto stable $\{111\}$ -faceted top and bottom faces of AgNPs via an Ostwald ripening process.^{11,18} In this regard, it is noticeable that very small nanoparticles were frequently identified in the TEM images of AgNPs during the reshaping process, whereas no small particle was observed after the completion of the process (Figure 1c). This anisotropic etching and redeposition of Ag mediated by Br^- reshaped the AgNPs toward AgNOs with reduced lateral dimensions and augmented thickness (Figure 1d). XPS investigations of the AgNOs unambiguously revealed the presence of Br on the nanostructure surfaces (see Figure S2 in the Supporting Information), in support of the proposed reshaping mechanism. HRTEM measurements also revealed that the highly crystalline nature of the Ag nanostructures was retained during the reshaping process and the resultant AgNOs were enclosed dominantly by $\{111\}$ facets (see Figure S3 in the Supporting Information). This result further supported the suggested mechanism. Analogous results were obtained using other halide ions, such as Cl^- and I^- (see Figure S4 in the Supporting Information). However, F^- ions were not effective for reshaping the AgNPs due to weak interactions with the

surfaces of AgNPs (see Figure S4 in the Supporting Information).²⁷ The identity of the counteranion did not influence the shape transformation of the AgNPs. The use of other mono- or multivalent counter cations, such as K^+ and Ca^{2+} , gave identical results. AgNPs with different edge lengths and thicknesses could also be reshaped into AgNOs through anisotropic etching with Br^- (see Figure S5 in the Supporting Information). We chose Br^- as the etchant and AgNPs with the above structural parameters as the starting materials for subsequent studies of the fabrication of tunable plasmonic substrates because this combination was shown to be effective in controlling the process time and tuning of the LSPR features.

The reshaping of AgNPs could be utilized for the fabrication of plasmonic structures on 2D substrates with tunable LSPR characteristics. AgNPs were assembled uniformly on amine-terminated substrates, such as glass, ITO glass, and Si wafers, which were prepared by the self-assembly of 3-APTMS on the substrates.^{21,28} Interactions between the substrates and the flat faces of AgNPs arranged the assembled AgNPs such that they were well-separated on the substrate in a face-down adsorption fashion. The amine-functionalized glass substrates coated with AgNPs appeared light blue and exhibited an intense LSPR peak at 626 nm. Immersion of the AgNP-coated substrate in an aqueous NaBr solution resulted in a gradual color change for the substrate from light blue to yellow. In line with the color change, the maximum peak position of the LSPR shifted from 605 to 426 nm (Figure 2). Control over the dipping time of the

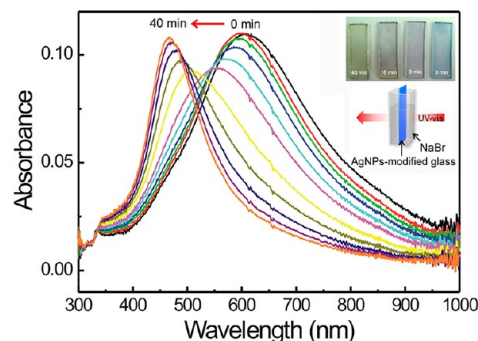


Figure 2. Successive extinction spectra (4 min interval) of AgNP-modified glass immersed in an aqueous NaBr solution (5.0×10^{-7} M). The upper inset shows digital photographs of AgNP-modified glass substrates obtained by controlling the dipping time into the NaBr solution.

substrate into the NaBr solution permitted the ready preparation of plasmonic substrates with different colors and LSPR features (upper inset of Figure 2). The changes in the plasmonic properties of AgNP-coated substrates were attributed to the reshaping of AgNPs on the substrate, as in solution. In fact, SEM studies of the substrates demonstrated that the shapes of the Ag nanostructures gradually changed from prism into oblate shapes with increasing immersion time in a NaBr solution (see Figure S6 in the Supporting Information).

This simple approach to fabricating tunable plasmonic substrates by reshaping NCs can also be used to prepare optical chips with gradient plasmonic properties. Vertical dipping of a AgNP-coated glass substrate into a NaBr solution with a predetermined dipping speed yielded a plasmonic substrate with a gradient of color and LSPR characteristics (Figure 3a). The formation of such plasmonic substrates was attributed to the creation of a gradient contact time with Br^-

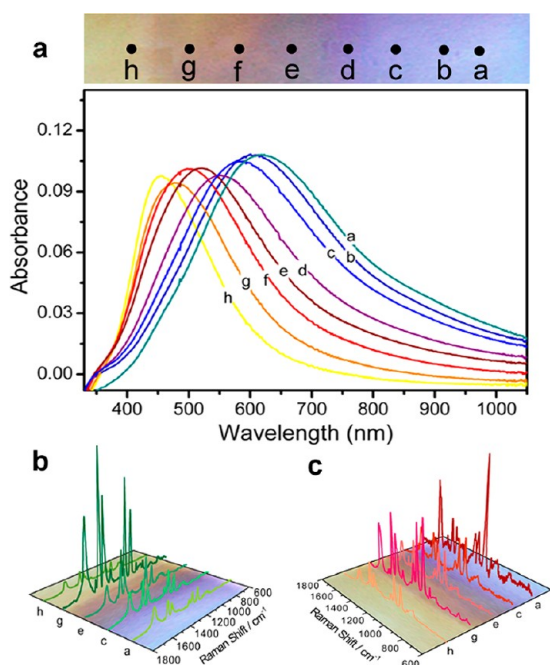


Figure 3. (a) Digital photograph and selected-area extinction spectra of a AgNP-coated glass substrate with gradient plasmonic properties, fabricated by dipping the substrate vertically into a NaBr solution (1.0×10^{-6} M) at a predetermined dipping speed (41 mm h^{-1}). The speed was controlled by a syringe pump to which the AgNP-coated glass substrate was attached. Each extinction spectrum was measured at the positions indicated in the photograph. SERS spectra of 4-ABT adsorbed at various lateral positions on the substrate, as denoted in a by using (b) 514.5 and (c) 632.8 nm laser excitation.

ions along the dipping direction. The AgNPs at the bottom area were transformed into AgNOs over the longest period of contact with the NaBr solution, whereas the AgNPs near the top portion retained their shape. In between, the shape gradient was correlated with the gradient of the contact time with Br^- ions, yielding a range of plasmonic properties. This type of plasmonic substrate can be useful in optical and sensing applications that require a gradient of plasmonic characteristics. To test the capabilities of the prepared substrates for optical and sensing applications, we investigated the SERS properties of the substrates using 4-ABT as a model compound, because 4-ABT adsorbs strongly onto Ag substrates by forming Ag–S bond and the resulting SERS properties depend strongly on the structures of the underlying substrates.²¹ Panels b and c in Figure 3 show the SERS spectra of 4-ABT adsorbed onto the substrates using 514.5 and 632.8 nm laser excitation, respectively. It is worth noting that the SERS intensities depended substantially on the lateral position on the substrate and the variations of SERS intensity obtained with different laser excitation wavelengths showed the opposite trend. The tunable SERS activity arose from the area-dependent plasmonic characteristics of the substrate. SERS effects are widely recognized to result from enhanced localized electromagnetic fields owing to LSPR.²⁹ The LSPR bands of regions that exhibit a maximal SERS enhancement for each excitation largely overlap with the excitation wavelength and can, therefore, produce the largest enhancements in the SERS signal. These results suggest that our substrates with gradient plasmonic properties can serve as tunable SERS substrates and are

expected to provide potential applications in SERS-based detection and sensing.

Interestingly, the present method can enable us to prepare tunable plasmonic 3D substrates. By exposing a AgNP-coated silica gel to Br^- ions, multiple-colored silica gels could be synthesized in a single step (Figure 4). In this experiment,

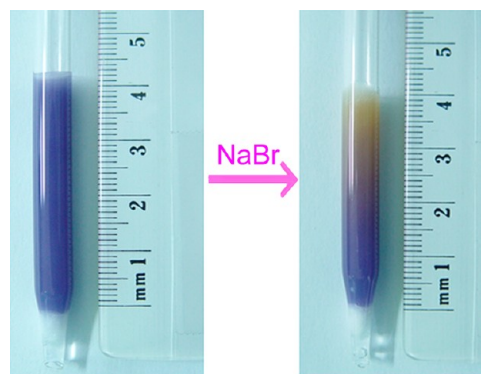


Figure 4. Digital photographs of a AgNP-coated silica gel packed into a glass column (left) before and (right) after exposure to an aqueous NaBr solution (1.0×10^{-6} M, 1 mL). In this experiment, AgNPs were assembled onto the surfaces of amine-functionalized silica gels by following the protocol used for preparing AgNP-coated glass substrates. The AgNP-coated silica gel was then packed into a glass column.

AgNPs were assembled onto the surfaces of amine-functionalized silica gels by following the protocol used for preparing AgNP-coated glass substrates. The AgNP-coated silica gel was then packed into a glass column. The passage of an aqueous NaBr solution through this column resulted in a color gradient along the column. As in the preparation of tunable plasmonic 2D substrates, the formation of a gradient color was caused by the gradient contact period of assembled AgNPs with Br^- ions associated with their positions along the column.

An appealing feature of the strategy developed in this work is that it can even allow the fabrication of 2D substrates with precisely controlled patterns of different plasmonic characteristics. Selective Br^- ion treatment of AgNP-coated substrates converted AgNPs in specific regions of substrates into AgNOs through a reshaping process, which thereby generates patterned plasmonic substrates. The patterned reshaping of AgNPs was achieved by μCP techniques,³⁰ i.e., a prepatterned PDMS stamp inked with NaBr was contact-printed onto a AgNP-coated substrate (Figure 5a). Typical optical micrographs of the cover glass substrates after processing are shown in Figure 5b, c. Circular and line patterns that differ in color from the background are clearly visible on the substrates, at which the NaBr was contact-printed. These features indicate the effective reshaping of AgNPs in a spatially controlled manner. The dimensions of the patterns were highly correlated with those on the PDMS stamp. A comparison of the SEM images obtained from the NaBr-printed regions with those obtained from the unprinted regions shows that the AgNPs were transformed into AgNOs only on the NaBr-printed regions (see Figure S7 in the Supporting Information). Interestingly, through a simple writing of NaBr solution with a brush on the AgNP-modified glass, plasmonic substrate with a free pattern could also be generated (Figure 6). These types of patterned plasmonic substrates cannot be achieved easily using conventional lithographic and patterning techniques, and will benefit a

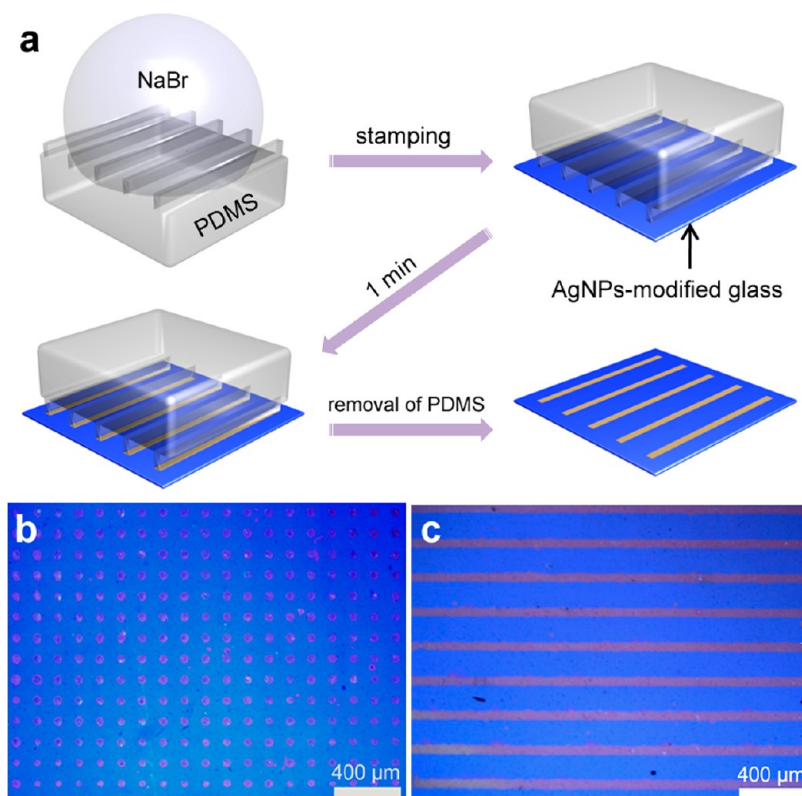


Figure 5. (a) Schematic illustration of the fabrication of patterned plasmonic substrates through μ CP of NaBr onto a AgNP-coated substrate. Optical micrographs of the AgNP-coated cover glass substrates after stamping of NaBr using PDMS stamps with (b) circular ($50\ \mu\text{m}$ cylinder separated by $150\ \mu\text{m}$) or (c) line patterns ($50\ \mu\text{m}$ line separated by $200\ \mu\text{m}$).

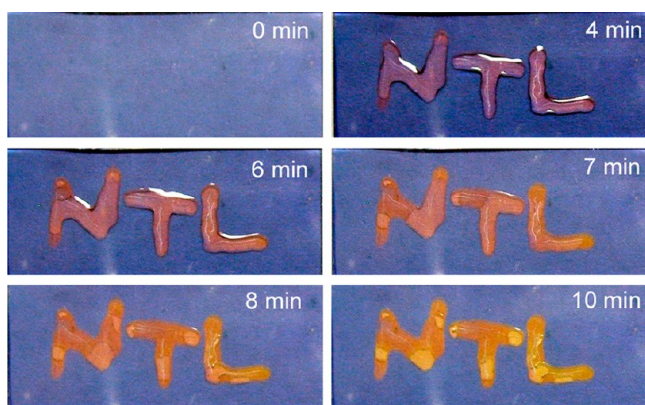


Figure 6. Digital photographs of a AgNP-coated glass substrate for different lengths of time after writing of an aqueous NaBr solution ($1.0 \times 10^{-5}\ \text{M}$) with a brush.

number of optical and sensing applications. For example, Pompa et al. demonstrated that spatial manipulation of the metal-enhanced fluorescence process could be achieved by using controlled patterns of metal nanostructures.³¹

CONCLUSIONS

Tunable plasmonic substrates could be fabricated by reshaping of metal nanocrystals. Anisotropic etching and redeposition of Ag atoms mediated by halide ions transformed Ag nanoprisms deposited on two- or three-dimensional surfaces or in solution into nanostructures with an oblate spheroidal shape, and corresponding localized surface plasmon resonances features could be tuned. The reshaping nanocrystal strategy can even

facilitate the preparation of new classes of plasmonic substrates with gradient or patterned plasmonic properties, which cannot be realized easily using existing lithographic techniques. The low-temperature mild chemical conditions of the present approach can provide a facile and promising route to the manufacture of tunable plasmonic structures on a variety of soft materials, such as gels and flexible polymer substrates. Further improvements and optimization of plasmonic properties, such as the widening of tunable range of LSPR feature can be achieved by tailoring the dimensions of the starting AgNPs. Our method can also be applied to other anisotropic metal nanostructures with different morphologies and compositions.

ASSOCIATED CONTENT

Supporting Information

Additional experimental data (Figure S1–S7). This material is available free of charge via the Internet at <http://pubs.acs.org>.

AUTHOR INFORMATION

Corresponding Author

*E-mail: sangwoohan@kaist.ac.kr

Notes

The authors declare no competing financial interest.

ACKNOWLEDGMENTS

This work was supported by Basic Science Research Programs (2010-0029149), EPB Center (2008-0062042), Future-based Technology Development Program (Nano Fields) (2009-0082640), and WCU Program (R31-2008-000-10071-0) through the National Research Foundation (NRF) funded by the Korean government (MEST), and was also supported by

the Industrial Core Technology Development Program by the Ministry of Knowledge Economy (10037397). The authors thank Y. Bae for contribution to preliminary experiments.

■ REFERENCES

- (1) Goesmann, H.; Feldmann, C. *Angew. Chem., Int. Ed.* **2010**, *49*, 1362.
- (2) Nie, Z.; Petukhova, A.; Kumacheva, E. *Nat. Nanotechnol.* **2010**, *5*, 15.
- (3) Lim, D.-K.; Jeon, K.-S.; Kim, H. M.; Nam, J.-M.; Suh, Y. D. *Nat. Mater.* **2010**, *9*, 60.
- (4) Barnes, W. L.; Dereux, A.; Ebbesen, T. W. *Nature* **2003**, *424*, 824.
- (5) Tao, A.; Sinsermsuksakul, P.; Yang, P. *Nat. Nanotechnol.* **2007**, *2*, 435.
- (6) Fan, J. A.; Wu, C.; Bao, K.; Bao, J.; Bardhan, R.; Halas, N. J.; Manoharan, V. N.; Nordlander, P.; Shvets, G.; Capasso, F. *Science* **2010**, *328*, 1135.
- (7) Tao, A. R.; Habas, S. E.; Yang, P. *Small* **2008**, *4*, 310.
- (8) Xia, Y.; Xiong, Y.; Lim, B.; Skrabalak, S. E. *Angew. Chem., Int. Ed.* **2009**, *48*, 60.
- (9) Kneipp, K.; Kneipp, H.; Kneipp, J. *Acc. Chem. Res.* **2006**, *39*, 443.
- (10) Mulvihill, M. J.; Ling, X. Y.; Henzie, J.; Yang, P. *J. Am. Chem. Soc.* **2010**, *132*, 268.
- (11) An, J.; Tang, B.; Zheng, X.; Zhou, J.; Dong, F.; Xu, S.; Wang, Y.; Zhao, B.; Xu, W. *J. Phys. Chem. C* **2008**, *112*, 15176.
- (12) Cathcart, N.; Frank, A. J.; Kitaev, V. *Chem. Commun.* **2009**, 7170.
- (13) Zhang, Q.; Ge, J.; Pham, T.; Goebel, J.; Hu, Y.; Lu, Z.; Yin, Y. *Angew. Chem., Int. Ed.* **2009**, *48*, 3516.
- (14) Chen, Y.; Wang, C.; Ma, Z.; Su, Z. *Nanotechnology* **2007**, *18*, 325602.
- (15) Lee, B.-H.; Hsu, M.-S.; Hsu, Y.-C.; Lo, C.-W.; Huang, C.-L. *J. Phys. Chem. C* **2010**, *114*, 6222.
- (16) Ni, W.; Kou, X.; Yang, Z.; Wang, J. *ACS Nano* **2008**, *2*, 677.
- (17) Liu, Y.; Mills, E. N.; Composto, R. J. *J. Mater. Chem.* **2009**, *19*, 2704.
- (18) Rodríguez-Lorenzo, L.; Romo-Herrera, J. M.; Pérez-Juste, J.; Alvarez-Puebla, R. A.; Liz-Marzán, L. M. *J. Mater. Chem.* **2011**, *21*, 11544.
- (19) Wu, H.-Y.; Liu, M.; Huang, M. H. *J. Phys. Chem. B* **2006**, *110*, 19291.
- (20) Métraux, G. S.; Mirkin, C. A. *Adv. Mater.* **2005**, *17*, 412.
- (21) Bae, Y.; Kim, N. H.; Kim, M.; Lee, K. Y.; Han, S. W. *J. Am. Chem. Soc.* **2008**, *130*, 5432.
- (22) Jin, R.; Cao, Y.; Mirkin, C. A.; Kelly, K. L.; Schatz, G. C.; Zheng, J. G. *Science* **2001**, *294*, 1901.
- (23) Jin, R.; Cao, Y. C.; Hao, E.; Métraux, G. S.; Schatz, G. C.; Mirkin, C. A. *Nature* **2003**, *425*, 487.
- (24) Noguez, C. *J. Phys. Chem. C* **2007**, *111*, 3806.
- (25) Pastoriza-Santos, I.; Liz-Marzán, L. M. *J. Mater. Chem.* **2008**, *18*, 1724.
- (26) Ciou, S.-H.; Cao, Y.-W.; Huang, H.-C.; Su, D.-Y.; Huang, C.-L. *J. Phys. Chem. C* **2009**, *113*, 9520.
- (27) Jiang, X. C.; Yu, A. B. *Langmuir* **2008**, *24*, 4300.
- (28) Xue, C.; Li, Z.; Mirkin, C. A. *Small* **2005**, *1*, 513.
- (29) Lu, Y.; Liu, G. L.; Lee, L. P. *Nano Lett.* **2005**, *5*, 5.
- (30) Xia, Y.; Whitesides, G. M. *Angew. Chem., Int. Ed.* **1998**, *37*, 550.
- (31) Pompa, P. P.; Martiradonna, L.; Della Torre, A.; Della Sala, F.; Manna, L.; De Vittorio, M.; Calabi, F.; Cingolani, R.; Rinaldi, R. *Nat. Nanotechnol.* **2006**, *1*, 126.